We are IntechOpen, the world's leading publisher of Open Access books
Built by scientists, for scientists

6,900
Open access books available

186,000
International authors and editors

200M
Downloads

Our authors are among the

154
Countries delivered to

TOP 1%
most cited scientists

12.2%
Contributors from top 500 universities

WEB OF SCIENCE™

Selection of our books indexed in the Book Citation Index
in Web of Science™ Core Collection (BKCI)

Interested in publishing with us?
Contact book.department@intechopen.com

Numbers displayed above are based on latest data collected.
For more information visit www.intechopen.com

Optical Storage Phosphors and Materials for Ionizing Radiation

Hans Riesen and Zhiqiang Liu
The University of New South Wales,
Australia

1. Introduction

Over recent years there has been significant progress in the development of optical storage phosphors and materials for ionizing radiation, resulting in important applications in the fields of dosimetry and computed radiography. The aim of this Chapter is to provide some background information as well as an overview of a range of modern storage phosphors and materials and their applications in dosimetry and computed radiography. Dosimetry is the measurement of absorbed dose of ionizing radiation by matter or tissue and is measured in the SI unit of gray (Gy) or sievert (Sv), respectively, where 1 Gy and 1 Sv are equal to 1 joule per kilogram. It is noted here that the non-SI units of rad (absorbed radiation dose; for matter) and rem (Roentgen equivalent in man; for tissue) are still heavily used; their conversions are given by 1 Gy=100 rad and 1 Sv=100 rem. A dosimeter allows us directly or indirectly to measure exposure, kerma, absorbed or equivalent dose and associated rates of ionizing radiation. A dosimetry system consists of the actual dosimeter and an associated reader. A dosimeter is characterized by its accuracy and precision, linearity, energy response, dose and dose rate dependence, spatial resolution and directional dependence.

It is well documented that even low doses of ionizing radiation can induce cancer. Thus personal radiation monitoring, i.e. dosimetry applied to people, has become highly important in recent years as the number of potential radiation sources is ever increasing. Radiation monitoring will also become more important in medical diagnostics and in radiation therapy as regulations become stricter. Nuclear accidents, such as the recent events in Fukushima, Japan, have highlighted the need for inexpensive and effective radiation monitoring systems that can be deployed to a large population. We note here that, of course, the exposure to natural background radiation is, to a great extent, unavoidable. For example, the average annual radiation dose per capita from natural and medical sources is 2.0 mSv/year and 2.8 mSv/year in Australia and the United Kingdom, respectively. The amount of radiation exposure is a function of geography and building standards. For example, in European homes there is a relatively high level of radon as the internal walls are based on clay bricks. This is reflected in the fact that the average equivalent dose by radiation from radon progeny is 0.2 mSv/year and 1.4 mSv/year in Australia and the United Kindom, respectively.

Ionizing radiation has a wide range of applications such as in the sterilization of medical hardware and food, in medical diagnostics and radiotherapy and in technical and scientific imaging (Andersen et al., 2009; Dyk, 1999; Eichholz, 2003; Mijnheer, 2008; Podgorsak, 2005;

Riesen & Piper, 2008). For safety and quality assurance, reliable radiation monitoring systems (dosimetry) are mandatory for these applications (Mijnheer, 2008). Dosimetry systems that are currently used for evaluating dose and its distribution include (Dyk, 1999; Mijnheer, 2008; Podgorsak, 2005; Schweizer et al., 2004):

1. Ionization chambers and electrometers for the determination of radiation dose. The standard chambers are either cylindrical or parallel plates. Active volumes for cylindrical chambers are between 0.1 and 1 cm^3 i.e. they are relatively bulky. Ionization chambers allow an instant readout, are accurate and precise and are recommended for beam calibration. Disadvantages include the fact that they have to be connected by cables and are relatively bulky i.e. they, in general, do not allow point measurements.

2. Standard radiographic films are based on radiation sensitive silver halide emulsions in thin plastic films. Exposure to ionizing radiation leads to a latent image in the film that can be read out by measuring the optical density variations within the film. Since the films are very thin they do not perturb the beam. However, the photosensitive silver halide grains in the film are rapidly saturated with a low number of X-ray photons i.e. the dynamic range of the blackening process is very limited. Nevertheless, due to the thin film thickness which limits scattering effects, the spatial resolution of this method is still one of the highest up to date. A dark room processing facility is required to work with radiographic film and they also need proper calibration.

3. Radiochromic film is based on polymer films that contain dye molecules that polymerize upon exposure to ionizing radiation. For example, GafChromic® film yields a blue coloration due to the radiation induced polymerization to polyacetylene. The film can be read out by a standard scanner.

4. Thermoluminescence is based on thermally excited phosphorescence of a range of systems. Sensitive materials include $CaSO_4$:Dy, CaF_2:Dy and LiF:Mg,Ti. The most commonly used thermoluminescence (TL) dosimeters in radiotherapy include the tissue-equivalent LiF:Mg,Cu,P and LiF:Mg,Ti. TL dosimeters can come in all forms and sizes and allow high spatial resolution e.g. they are suitable for point dose measurements. However, TLD requires relatively complex reader units and hence instant readout is not possible. Moreover, the information is destroyed upon readout and can, in general, easily be lost.

5. Silicon diode and MOSFET (metal-oxide-semiconductor-field-effect-transistor) based dosimetry offer the advantages of small size, instant readout and high sensitivity but require that cables are connected. Also, their sensitivity changes with accumulated dose i.e. results are not very reproducible.

6. Optically stimulated (or photostimulated) luminescence (OSL or PSL) systems are related to TLD but require higher stimulation energy. In a typical OSL (PSL) material, such as BaFBr/Eu^{2+}, red light stimulates the recombination of electrons and holes that were created by exposure to ionizing radiation, yielding broad blue luminescence light. OSL materials offer high spatial resolution and sensitivity but are susceptible to ambient light and therefore data can be inadvertently lost. An OSL material that has been used in vivo fibre based dosimetry is the Al_2O_3:C system by Landauer. In this case, the blue emission is stimulated by green light (e.g. Nd:YAG laser at 532 nm). However, the size of the crystal required for this system is still relatively large (2x0.5x0.5 mm^3) and the material loses its information under ambient lighting conditions.

7. Electronic Portal Imaging Devices (EPIDs), based on amorphous silicon, are used for real time acquisition of megavolt images during patient treatment and can be, to some

extent, used to undertake dosimetry. Disadvantages of these devices include the fact that they are not linear with dose and dose rate and they are also relatively bulky and need to be connected with cables etc.

Storage phosphors can also be used as two-dimensional dosimeters, i.e. some spatial information about radiation exposure can be derived. This, of course, is based on computed radiography which is another important application of storage phosphors. The basic principle of computed radiography is illustrated in Figure 1.
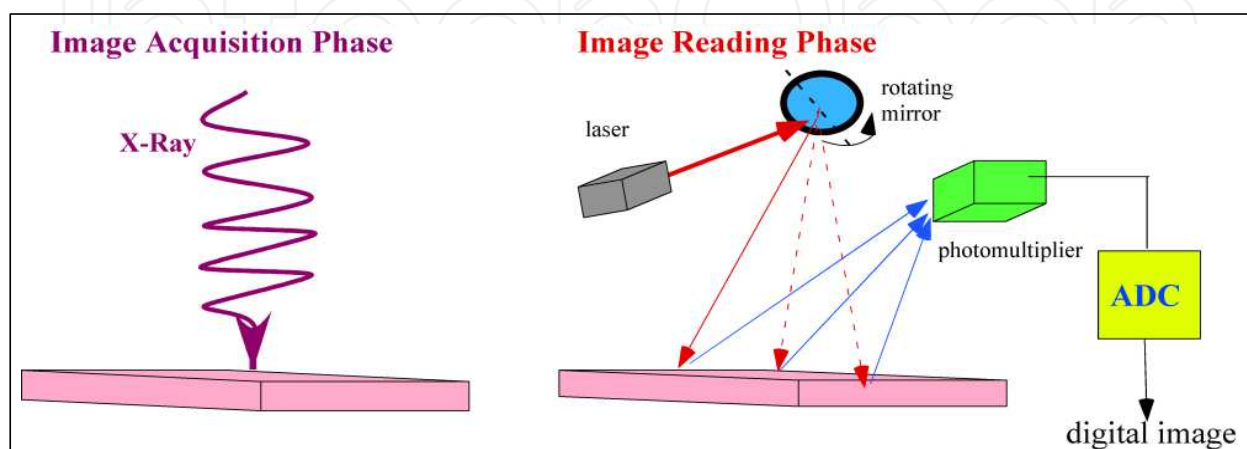
Fig. 1. Principle of computed radiography. An object on top of an imaging plate is exposed to X-rays. The storage phosphor renders a latent image of the object via the distribution of absorbed dose. The absorbed dose is measured in the reading phase and the signal is digitized. The readout for the conventional storage phosphor is undertaken by the so-called "flying-spot" method.

Since its introduction in the early 1990s, the method of computed radiography has gained significant momentum since it allows a reduction of the dose to as low as 18% in comparison with screen-film technology. In conventional computed radiography (CR), the latent image on an imaging plate (comprising of an X-ray storage phosphor) formed by exposure to ionizing radiation, is read out by photostimulated (optically stimulated) emission by using the so-called "flying-spot" method. In this method a focused red helium-neon laser beam is scanned across the imaging plate and the resulting photostimulated emission in the blue-green region of the visible spectrum as measured by a photomultiplier is converted into a digital signal pixel-by-pixel. In contrast to the screen-film method, computed radiography phosphors enable a dynamic range of up to eight orders of magnitude. However, the spatial resolution of imaging plates in CR is not yet on a par with screen-film technology due to the relatively large crystallites/grain size required in the commercially used photostimulable X-ray storage phosphor, $BaFBr(I):Eu^{2+}$ (Nakano et al., 2002; Paul et al., 2002).

In this chapter, an overview of some optical storage phosphors and materials is given and storage mechanisms and applications are briefly discussed with emphasis on a novel class of photoluminescent storage phosphors.

2. Optical storage phosphors and materials

We define an optical storage phosphor or material to be a system that undergoes some electronic or structural change that allows an optical readout of radiation dose. This definition encompasses thermoluminescence where glow curves are measured upon heating

the thermoluminescent material that was exposed to ionizing radiation, photostimulated (optically stimulated) luminescence where the stored energy is released upon stimulation by light, radiochromic film where chemical species are created that can be read out by absorption spectroscopy, or photoluminescent or radio-photoluminescent phosphors where the radiation induced centres are metastable or stable and can be repetitively read out by photoexciation. Silver-based emulsions are also optical storage media in the broader sense, as the darkening of the film can be read out quantitatively by the change of optical density. However, such films are not discussed here in detail. Our definition of what constitutes an optical storage phosphor or material is schematically depicted in Figure 2.
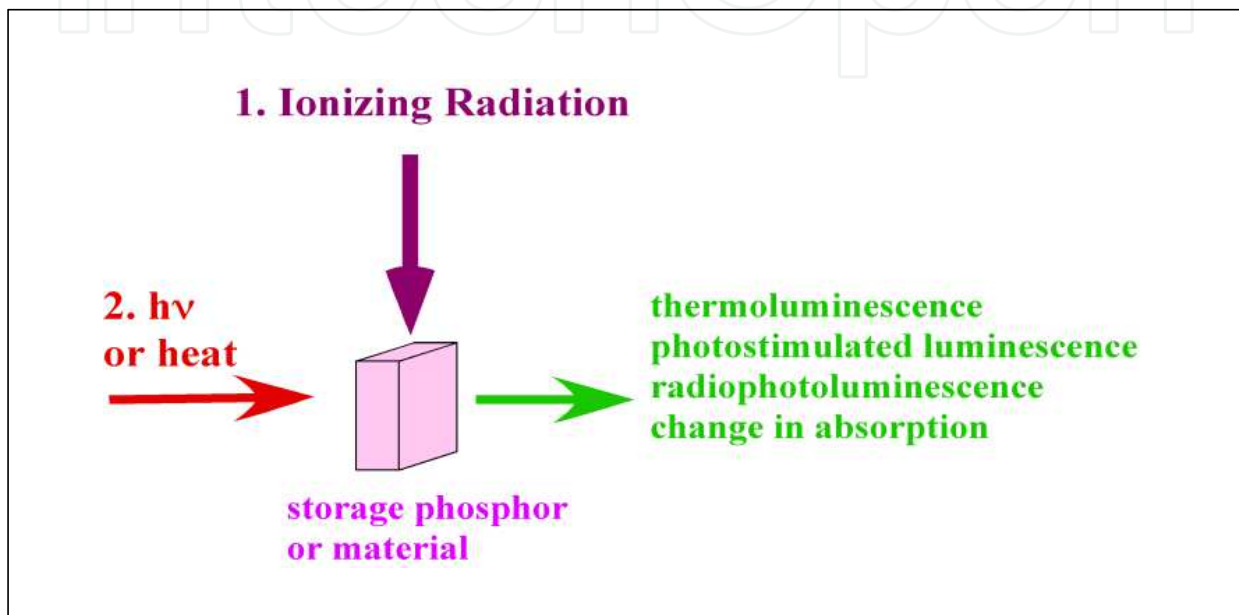

Fig. 2. General principle of an optical storage phosphor. Ionizing radiation leads to electronic and/or structural modifications in a material and the associated changes can be measured by luminescence or absorption spectroscopy.

The general mechanism of materials that exhibit thermoluminescence or photostimulated luminescence is schematically illustrated in Figure 3. Upon exposure to ionizing radiation, electron-hole pairs are created and the electrons and holes are subsequently trapped at defect sites within the crystal lattice or self-trapped such as by the creation of the V_k-centre. For example, electrons can be trapped at anion-vacancies such as F, Cl or I vacancies in halide crystals, forming the so-called F-centres (F stands for Farbe which is the German word for colour) which display oscillator strengths of close to unity. Holes can be self-trapped by the well-known V_k centres, e.g. a hole can be shared between two adjacent halide ions, leading to significant lattice distortion, which in turn may immobilise the hole to a certain extent. In thermoluminescent materials the electrons are liberated by heating the material since the electron traps are relatively shallow and the conduction band is thermally accessible. In photostimulable (optically stimulable) materials the electron trap is deeper and higher energies are required to liberate the electron. Upon the liberation of the electron it can combine with the hole leading to emission of light, either directly through the recombination process or by transferring excitation energy to an activator centre such as Eu^{2+} or the like.
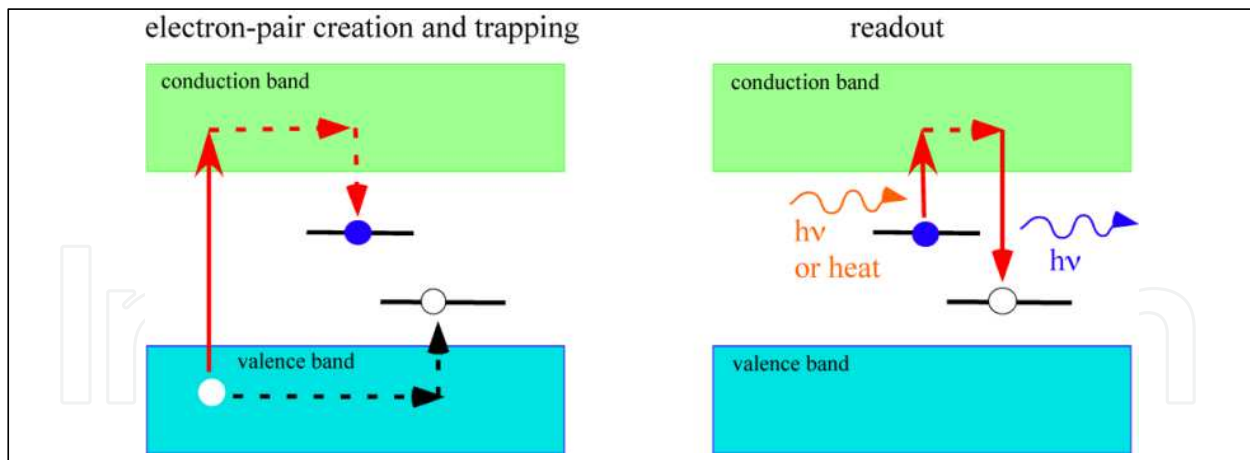
Fig. 3. Schematic diagram of the main mechanism of materials that display thermoluminescence or optically stimulated luminescence after exposure to ionizing radiation. Electrons and holes created by ionizing radiation are trapped out. Subsequently, heat or light can liberate electrons back into the conduction band and after recombination with the hole light is either emitted directly or by the transfer of the exciton energy to an activator such as a transition metal ion or a rare earth ion.
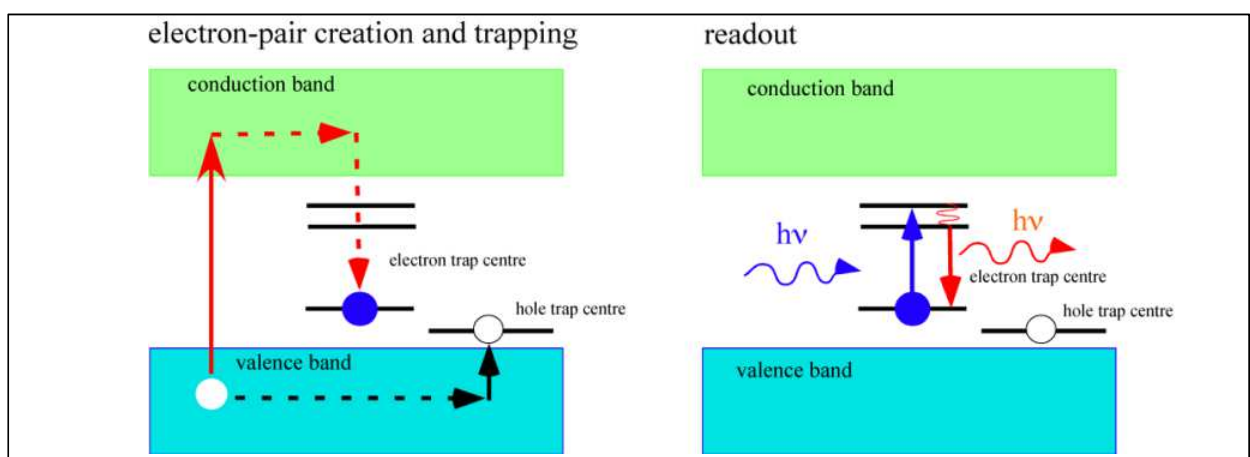

Fig. 4. Schematic and simplified diagram of the main mechanism of materials that display radiophotoluminescence after exposure to ionizing radiation. Electrons are localized in deep traps, e.g. transition metal ions, F-centres, rare earth ions. The electron trap centres can then be repetitively photoexcited from the electronic ground state to an electronically excited state. The electronically excited state is then deactivated by the emission of light and the centre induced by ionizing radiation is conserved.

In materials that display photoluminescence or radiophotoluminescence, electrons promoted to the conduction band by ionizing radiation migrate to deep traps. This is illustrated in Figure 4. These deep traps may be rare earth or transition metal ions doped as impurities into a wide bandgap host. The reduced trap can then be photoexcited without that the electron is promoted back into the conduction band. Naturally, if high light intensities are used, the electron may be promoted back into the conduction band by a two-step photoionization process. It is also possible that the excited state is close to the conduction band and hence some electrons will be liberated thermally from these excited

states. However, in contrast to photostimulable materials, the signal in radiophotoluminescent materials does not decrease under ideal conditions i.e. the material can be read out for a very extended period of time to render very high signal to noise ratios. We define a photoexcitable storage phosphor as a radiophotoluminescent material that can be restored to its initial state by processes such as two-step photoionization.

A major advantage of optical storage materials for ionizing radiation in comparison with electronic devices is the fact that they are always in the accumulation mode and no battery or electric power supply is needed. This is particularly important in dosimetry applications where it is required that a dosimeter is on at all times.

2.1 Radiochromic film

Since the 1980s, two-dimensional radiation detectors employing radiochromic films have been widely applied in ionizing radiation dosimetry and medical radiotherapy (Soares, 2007; 2006). Radiochromic films consist of a thin polyester base impregnated with radiation-sensitive organic microcrystal monomers. Upon ionizing radiation, the film emulsions undergo a colour change through a chemical reaction (usually polymerization) and the radiation response signal can be read out by measuring the absorbance or optical density using spectrometers at certain wavelengths. Currently, the most popular radiochromic film in medical applications are the polydiacetylene based GafChromic® films designed by International Specialty Products (ISP). GafChromic® film was first introduced by Lewis (Lewis, 1986) and further developed by McLaughlin et al. at the National Institute of Standards and Technology (NIST) in the United States. Table 1 lists some current commercial GafChromic® films.

Application	Film type	Active Layer Thickness (μm)	Dose Range (Gy)	Spatial Resolution (dpi)	Energy Range
Radiotherapy	HD-810	6.7	10 ~ 2500	10,000	MV
	MD-55-2	67	10 ~ 100	5,000	MV
	RTQA2	17	0.02 ~ 8	5,000	MV
	EBT-2	30	0.01 ~ 40	5,000	kV-MV
	EBT-3	30	0.01 ~ 40	5,000	kV-MV
Radiology	XR-QA2	25	0.001 ~ 0.2	5,000	kV
	XR-CT2	25	0.001 ~ 0.2	5,000	kV
	XR-M2	25	0.001 ~ 0.2	5,000	kV
	XR-RV3	17	0.01 ~ 30	5,000	kV

Table 1. List of commercial GafChromic® films.

With different film implementations, the GafChromic® film exhibits a variety of dose responses in the energy range from keV to MeV, targeting different areas of medical radiotherapy. For example, with only a 6.7 μm thick active layer, the transparent GafChromic® HD-810 film is predominantly employed in high dose radiation measurements with doses up to 2500 Gy. In contrast, by adding a yellow dye into the sensitive layer, the latest GafChromic® EBT film is designed mainly for radiotherapy applications. Many studies have been devoted to the characterization and performance assessment of the GafChromic® films including the dose response functions (sensitivity), film stability and image resolution (Arjomandy et al., 2010;

Rink et al., 2008; Secerov et al., 2011). In addition to GafChromic® films, other commercial radiochromic films include FWT-60 from Far West Technology Inc., the B3 dosimetry lines manufactured by the Gex Corporation and the SIRAD (Self-indicating Instant Radiation Alert Dosimeter) developed by Gordhan Patel at JP Laboratories (Mclaughlin et al., 1991). Compared with conventional silver halide based photographic films, the radiochromic film offer many advantages in medical dosimetry and radiography, such as outstanding spatial resolution (>1200 lines/mm for GafChromic® film (Secerov et al., 2011), accurate and precise dose measurements, weak energy dependence and relatively easy handling.
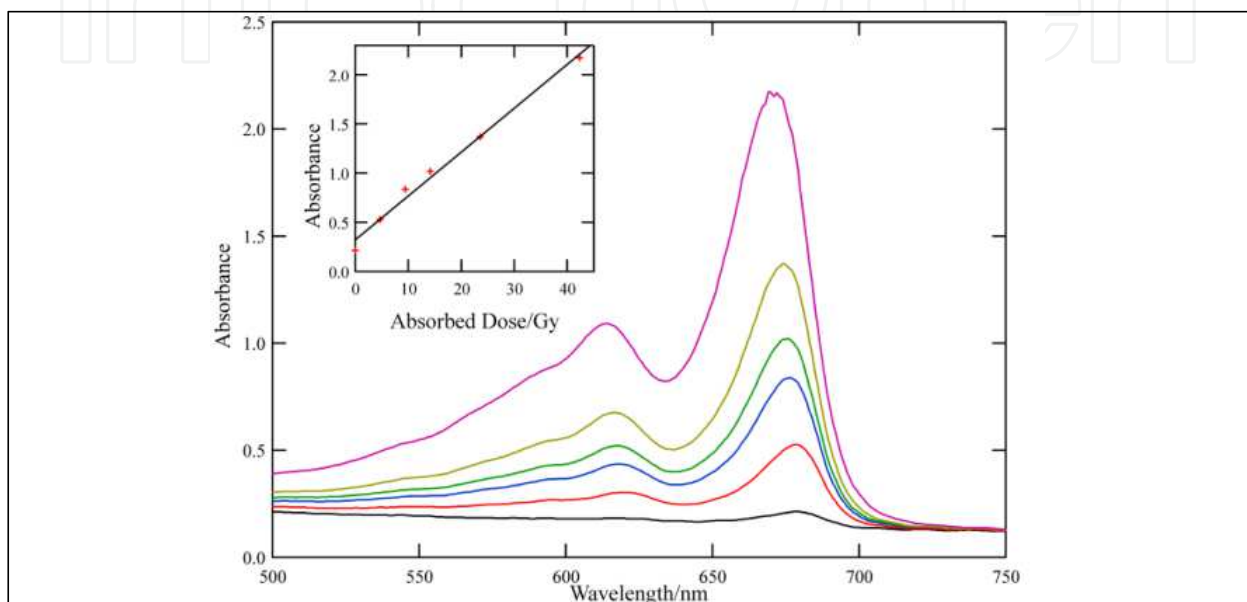
Fig. 5. Absorption spectra of GafChromic® film HD-810 as a function of high X-ray dose (40 kVp). The inset shows a plot of the absorbance at 676 nm of the film as a function of the absorbed dose. The absorption spectra were measured on a Cary-50 UV-Vis absorption spectrometer.
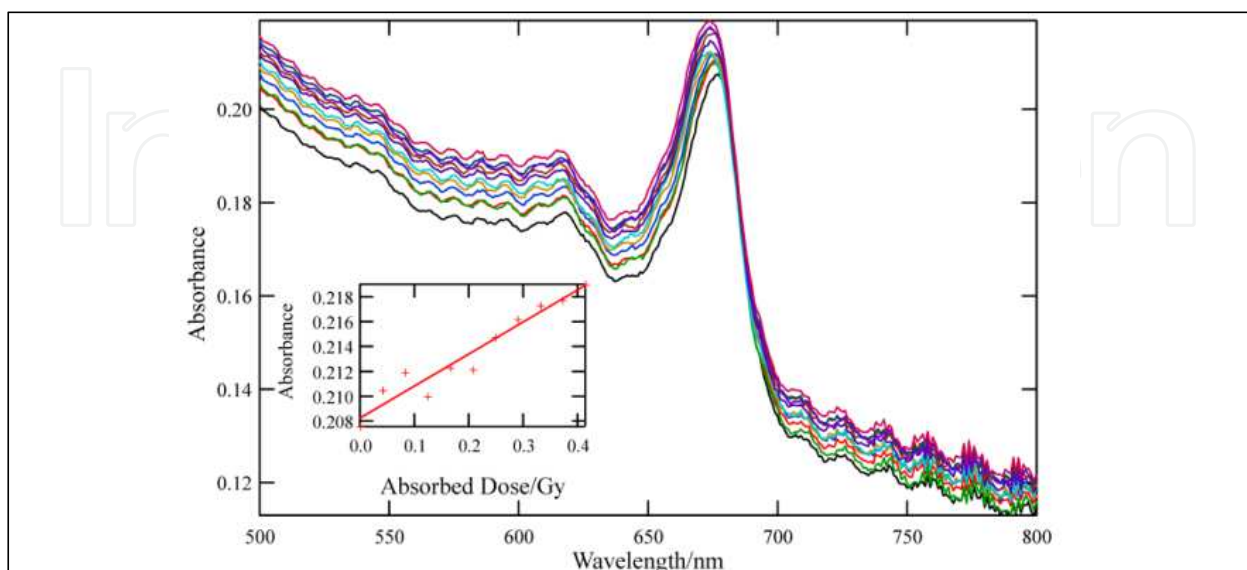

Fig. 6. As in Figure 5 but for low X-ray dose and 60 kVp radiation.

Figures 5 and 6 illustrate the X-ray dose dependence of the absorption spectra of GafChromic® film HD-810 at high and low doses, respectively. The optical absorbance at 676 nm of the film increases linearly in the dose range of 0.04 Gy to 2 Gy of X- irradiation. Weak energy dependence is another desirable property for a two-dimensional radiation detector in order to obtain accurate values of absorbed doses.

Due to the high atomic number components in silver–based film emulsions, the conventional photographic films suffer from a strong photon energy dependence of the response to dose. This has been significantly improved by radiochromic film dosimetry. Buston et al. (Butson et al., 2010) examined the energy dependence of the GafChromic® EBT2 film dose response in the X-ray range of 50 kVp to 10 MVp and a 6.5% ± 1% variation in optical density to absorbed dose response was obtained. The near energy-independence of radiochromic film has made it an ideal technology in some medical applications where a broad energy range of radiation sources is delivered. Furthermore, unlike the photographic films, the radiochromic films do not require subsequent chemical processing and can produce repetitive responses over a relatively long period of time. Despite the numerous advantages, special attention has to be paid to the environmental factors such as temperature, humidity and UV exposure in the irradiation and readout processes of the radiochromic films. Abdel-Fattah and Miller (Abdel Fattah & Miller, 1996) have investigated the effects of temperature during irradiation on the dose response of the FWT-60-00 and B3 radiochromic film dosimeters. At temperatures between 20 and 50 °C and a relative humidity between 20 and 53%, the temperature dependences of FWT-60-00 and Risø B3 dosimeters were found to be 0.25 ± 0.1% per °C and 0.5 ± 0.1% per ° C, respectively. For the GafChromic® films, it was suggested to be best stored in the dark at the temperature of ~22ºC (Mclaughlin et al., 1991).

2.2 Thermoluminescent materials

Thermoluminescence (TL) is the emission of light produced by heating of a material. The phenomenon of thermoluminescence has been known for a long time and has been reported by Robert Boyle as early as 1663 when he observed thermoluminescence from diamond (Horowitz, 1984). At the end of the 19th century Borgman (Borgman, 1897) reported that X-rays and radioactive substances can induce thermoluminescence in particular materials. However, it was only in 1953 when Daniels et al. suggested the application of thermoluminescence in the field of dosimetry (Daniels et al., 1953). The early work was mostly involving the tissue equivalent LiF but also Al_2O_3. From the 1960s onwards thermoluminescence was regarded to be a viable alternative to film dosimetry and LiF became the TLD-100 standard after Harshaw purified the material and refined the crystal growth to make the properties of the material more reproducible. LiF is still in use today but the main key is to select a material for a specific monitoring application. Up to this date dosimetry based on thermoluminescence is still the main mode of personal radiation monitoring, with a plethora of suitable materials for a wide range of applications.

The mechanism of thermoluminescence induced by radiation is generally described in the following way. Upon ionizing radiation, free electron and hole pairs are created due to the photoelectric effect. The electrons and holes are then captured at different defect centres (electron and hole traps) within the material. During the subsequent heating process, the trapped electrons are released and recombine with the trapped holes, resulting in emission of light with the intensity proportional to the absorbed ionizing radiation dose (see Figure 4

above). Compared with other radiation dose measurement techniques, thermoluminescence dosimetry offers many advantages, such as a relatively small dosimeter size, high sensitivity over a wide range of surface dose levels from μGy to several Gy, long-term information storage and versatile applications in different types of radiation including X-rays, γ and β rays and neutrons.

There are a large number of materials exhibiting thermoluminescence, mostly insulators or semiconductors containing lattice defects resulted from substitutional impurities or ionizing irradiation. However, not all the materials with thermoluminescence properties are suitable for radiation dosimetry. There are several requirements for the practical use of thermoluminescence materials in radiation measurements (Kortov, 2007). For example, it is desirable that the material has a simple glow curve with the main peak occurring at around 200 °C. If thermoluminescence is also induced at lower temperatures, the thermal energy at room temperature may be high enough to liberate trapped electrons and fading can occur. On the other hand, when the glow curve is complex on the high-temperature side, the stored energy remaining after the radiation measurement has been performed, has to be dissipated (Yen et al., 2007). Figure 7 shows the glow curve of LiF:Mg, Cu, P (Bos, 2001; McKeever et al., 1993) after exposed to 0.4 Gy ^{60}Co ·-radiation. From this figure it follows that dosimeters based on this material should not be subject to temperatures above 80 °C, otherwise fading starts to occur. In addition to a simple glow curve, a linear dose response, high luminescence efficiency, low photon energy dependence and long term stability are also desirable for the application of thermoluminescent materials in radiation dosimetry (Azorin et al., 1993).
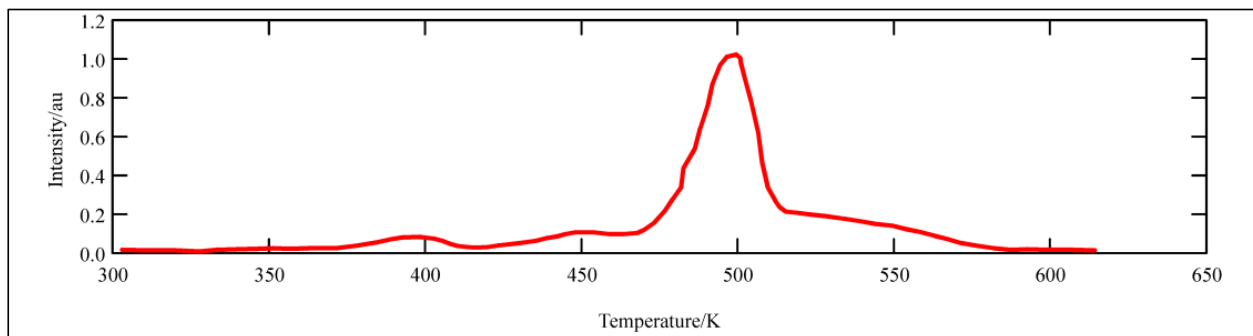

Fig. 7. Glow curve of LiF:Mg, Cu, P (TLD-100H). Thermal annealing procedure: 10 min at 240 °C with a heating rate of 2.1 °C /s followed by cooling in air. The absorbed dose was 0.4 Gy from a ^{60}Co source. The main dosimetric peak occurs at ~200 °C.

Table 2 lists some typical commercial thermoluminescence dosimeters with their applications and useful dose ranges. These commercial dosimeters generally exhibit emission at 380 - 480 nm, which falls off in the spectral response range of common photomultipliers. The thermoluminescence peak is located from 180 °C to 260 °C, offering an easy readout process. With an effective atomic number (Z_{eff}) close to that of soft biological tissue, LiF-based dosimeters are the most widely used thermoluminescence phosphors in personal radiation monitoring due to its very low photon energy dependence (Azorin et al., 1993). However, the glow curves of LiF-based dosimeters consist of at least seven peaks (Satinger et al., 1999). In contrast, CaF$_2$:Mn and Al$_2$O$_3$:C dosimeters offer simpler glow curves and higher sensitivity (Kortov, 2007). Nakajima et al. (Nakajima et al., 1978) first introduced the LiF:Mg, Cu, P (TLD-100H) which shows a 15 times greater sensitivity than that of the LiF:Mg, Cu (TLD-100). Furthermore, to improve the sensitivity of the dosimeters

to thermal neutrons, [6]Li and [7]Li isotope based LiF dosimeters were designed to measure thermal neutrons in a mixed radiation field (Azorin et al., 1993).

Material	Dosimeter	Z_{eff}	Application	Useful Range
LiF:Mg, Ti	TLD-100	8.2	medical physics	10 μGy - 10 Gy
CaF_2:Dy	TLD-200	16.3	Environmental	0.1 μGy - 10 Gy
CaF_2:Tm	TLD-300	16.3	Low dose gamma rays	0.1 μGy - 10 Gy
CaF_2:Mn	TLD-400	16.3	Environmental	0.1 μGy - 100 Gy
Al_2O_3:C	TLD-500	10.2	Personnel	0.05μGy - 10 Gy
[6]LiF:Mg, Ti	TLD-600	8.2	Neutron and gamma rays	10 μGy - 10 Gy
[7]LiF:Mg, Ti	TLD-700	8.2	Gamma rays and thermal neutron	10 μGy - 10 Gy
LiB_4O_7:Mn	TLD-800	7.4	High dose and neutron	450 ・Gy-10^4 Gy
$CaSO_4$:Dy	TLD-900	15.5	Environmental	1 μGy – 10^3 Gy
LiF:Mg, Cu, P	TLD-100H	8.2	Personnel	1 μGy - 20 Gy
[6]LiF:Mg, Cu, P	TLD-600H	8.2	Personnel	1 μGy - 20 Gy
[7]LiF:Mg, Cu, P	TLD-700 H	7.4	Personnel	1 μGy - 20 Gy

Table 2. Examples of commercial thermoluminescence dosimeters.

One of the better performers is $CaSO_4$:Dy which is approximately 10 times more sensitive than LiF:Mg,Ti (TLD-100). This material offers a simple processing cycle and is typically suspended in a Teflon disc. Annealing of only 2 hours at a temperature of ~280ºC is required to erase the residual radiation induced thermoluminescence before the material can be reused. In contrast, LiF:Mg,Ti requires annealing of 5 hours at 300ºC, followed by 20 hours at 80ºC. However, CaF_2 and $CaSO_4$ based thermoluminescence materials are exceptionally light (UV) sensitive, and fading is enhanced significantly. These materials have to be handled, used and stored in opaque containers to avoid belaching of the thermoluminescence signal. Moreover, the reading accuracy depends on the heating rate and multiple readings are not possible as the stored energy is lost upon heating. Importantly, TL dosimeters cannot work in test-accumulation mode (multiple irradiation and reading). Also, the irradiation memory is dependent on the operation temperature. The precision on reuse is also lowered (±2% above 1 mSv and higher below this value) and the long term response retention is restricted (the best materials show 5% loss at room temperature for one year). A major drawback of thermoluminescence based dosimetry systems is the requirement of relatively complex reading instrumentation including a well-controlled flowing gas thermoelectric heating system (±1°C). Current thermoluminescence dosimeter manufacturers include the Solid Dosimetric and Detector Laboratory in China, Nemoto in Japan, the Institute of Nuclear Physics in Poland and Saint-Gobain Crystals and Detectors in the USA.

2.3 Photostimulable (optically stimulable) storage phosphors

As is illustrated in Figure 3, the mechanism of materials that show thermoluminescence and photostimulated (or optically stimulated) luminescence (PSL or OSL) is, to a great extent, the same but OSL (PSL) materials provide significantly deeper traps for the electrons and/or holes created upon exposure to ionizing radiation and hence thermal energies are not high enough to liberate the trapped electrons. Thus, in contrast to thermoluminescence, optically stimulated luminescence is an all-optical technique that does not require heating of the storage material. This allows much simpler and compact designs of reader units. The application of optically stimulable phosphors in dosimetry was first suggested in the 1950s. It was then initially mostly used for archaeological and geological dating, e.g the dating of quartz until the development of sensitive anion-deficient Al_2O_3:C. Photostimulable materials also became very important with the implementation of BaFBr:Eu^{2+} in computed radiography.

2.3.1 Al_2O_3:C

The Al_2O_3:C system has been extensively covered in a book by Bøtter-Jensen et al. (Botter-Jensen et al. 2003) and an elegant overview of the main features of this material is also given in a recent article by Akselrod (Akselrod, 2010). Anion-deficient α-Al_2O_3:C was firstly developed as a thermoluminescence material (Akselrod et al., 1990) but it was soon realized that it can serve as an OSL phosphor with excellent properties. In terms of its thermoluminescence properties, it is about 40-60 times more sensitive than LiF based TLD-100. However, the sensitivity is strongly dependent on the heating rate, complicating routine dosimetry measurements. In contrast, Al_2O_3:C appears to be an ideal material for optically stimulated luminescence. Neutral and charged oxygen vacancies (F, F^+) play an important part as luminescence centres. In particular, the presence of F^+ centres is important as they are the recombination centres for electrons, yielding excited F-centres. Al_2O_3:C displays a linearity of light output as a function of radiation dose over seven orders of magnitude. The long luminescence lifetime of 35 ms of the emitting F-centres allows simple time-dependent readout schemes and this has been implemented in so-called pulsed optically stimulated luminescence measurements (Akselrod et al., 1998) where the emitted light is only measured between the stimulating light pulses in order to reduce the requirement for heavy optical filtration. The system is now fully commercialized by Landauer with a suite of dosimetry products that allow static and dynamic monitoring of ionizing radiation. Landauer also offers a portable reader unit. A drawback of the Al_2O_3:C material is the fact that it has to be kept in light-tight containers, otherwise the stored energy is rapidly erased by visible light.

2.3.2 BaFBr(I):Eu^{2+}

Excellent and detailed reviews of this material have been published by von Seggern (von Seggern, 1999) and Schweizer (Schweizer, 2001). BaFBr(I):Eu^{2+} is the most widely used storage phosphor in computed radiography, with a number of major companies that offer imaging plates and associated readers for medical imaging.

Current storage phosphors contain centres for the capture of X-ray generated electrons and holes. For the BaBrF:Eu^{2+} storage phosphor both the $F^+(Br^-)$ and the $F^+(F^-)$ defects can act as electron storage centres whereas the Eu^{2+} acts as the hole trap. Upon X-ray irradiation of the X-ray storage phosphor BaBrF:Eu^{2+} electron-hole pairs are created. The electrons and holes are trapped at anion vacancies and the Eu^{2+}, respectively, creating F-centres and Eu^{2+}/V_K-centres (a V_K-centre is a hole shared between two neighbouring halide anions). However,

some electron-hole pairs recombine spontaneously after their creation without being trapped and lead to spontaneous emission (scintillation). Upon excitation of the F-centres at 2.1 eV and 2.5 eV for the $F(Br^-)$ and $F(F^-)$ centres, respectively, the electrons recombine with the holes to form excitons. When the excitons are deactivated its excitation energy is resonantly transferred to the activator, Eu^{2+}, which in turn, leads to the broad $4f^65d \rightarrow 4f^7$ emission at about 390 nm. It was believed initially (Takahashi et al., 1984) that the hole combines with Eu^{2+} to form Eu^{3+}. However, there is evidence that this is not the case as follows, for example, from the fact that the Eu^{2+} photoluminescence does not decrease upon X-irradiation (Hangleiter et al., 1990; Koschnick et al., 1991). The exact mechanism of the electron–hole recombination is still controversially discussed; some experiments are at variance with a recombination of the electron-hole pairs via the conduction band. An alternative mechanism proposes a spatial correlation of the electron and hole traps and it is believed that recombination occurs via tunnelling of the electrons.
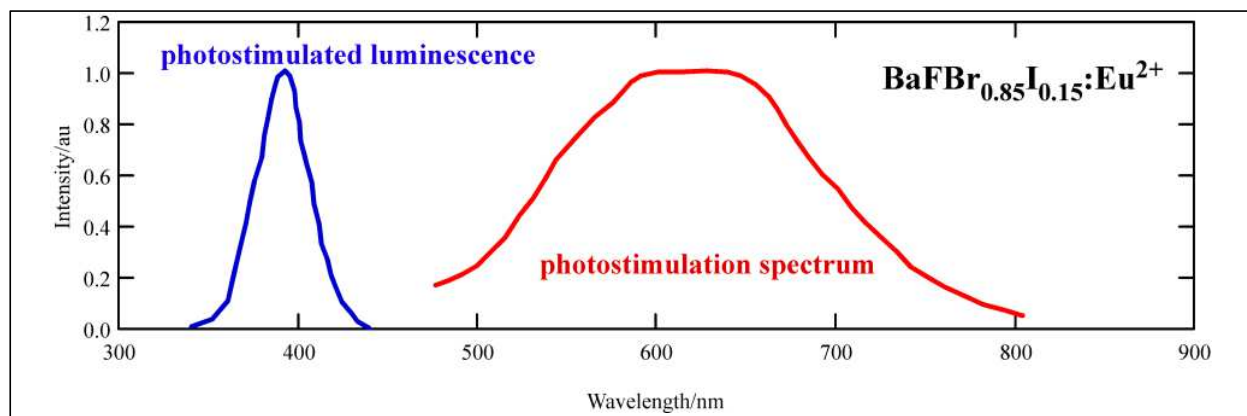

Fig. 8. Photostimulated luminescence and photostimulation spectra of $BaFBr_{0.85}I_{0.15}:Eu^{2+}$.

2.3.3 CsBr:Eu^{2+}

CsBr:Eu^{2+} displays significant photostimulated luminescence after X-ray exposure (Leblans et al., 2001; Schweizer et al., 2000) and its figure-of-merit as a storage phosphor is as high as for BaFBr(I):Eu^{2+} (Hackenschmied et al., 2002; Schweizer, 2001). In particular, this material can be grown in the form of needle crystals by vacuum deposition (Weidner et al., 2007), allowing an improved lateral resolution in comparison with BaFBr(I):Eu^{2+}. The sensitivity of this material appears to be strongly dependent on thermal treatment (Hackenschmied et al., 2003) and hydration (Appleby et al., 2009). In CsBr:Eu^{2+} the holes are trapped as V_K-centres in the vicinity of Eu^{2+}, and the electrons are trapped in F-centres and hence the spectroscopy of this system is very much related to the BaFBr:Eu^{2+} spectra with minor dielectric shifts of the spectra. However, poor radiation hardness appears to be a major problem with this material. In particular, the photostimulated luminescence deteriorates rapidly upon exposure to high X-ray dose and this deterioration is correlated with a reduction of the photoexcited Eu^{2+} fluorescence that has been attributed to an agglomeration of Eu^{2+} leading to luminescence quenching. (Zimmermann et al., 2005). This conclusion has been reached since no increase in Eu^{3+} luminescence is observed.

2.3.4 BeO

With near tissue equivalence (Z_{eff} = 7.1), relatively high sensitivity and low cost, beryllium oxide (BeO) has been well-documented as a thermoluminescence dosimetry (TLD) material

with a range of applications particularly in medical fields (McKeever, 1988; McKeever et al., 1995; Vij & Singh, 1997). One of the most popular forms of BeO-based TLD is Thermalox® 995. Modifications of the material can be found as BeO:Li (Yamashit et al., 1974), BeO:Na (Yamashit et al., 1974) and BeO:TiO$_2$ (Milman et al., 1996). Depending on the preparation methods and the type of radiation source, the glow curves of BeO-based TLD materials exhibit the main dosimetric peaks between 160 °C and 280 °C. Compared with other commercial thermoluminescence dosimetric systems, the main disadvantage of the BeO-based materials is the rapid light-stimulated thermoluminescence fading. Under laboratory fluorescent light, rapid fading of 50 % in 30 min for the thermoluminescence peak at 167 °C has been reported in several types of commercial BeO ceramic dosimeters (Crase & Gammage, 1975). Based on the characteristic light-sensitive thermoluminescence of BeO, Albrecht and Mandeville (Albrecht & Mandeville, 1956) first investigated optically stimulated luminescence of the X-ray irradiated BeO by using visible photons. Bulur and Göksu (Bulur & Göksu, 1998) examined the detailed dosimetric properties of Thermalox® 995 as optically stimulated luminescence dosimeter, such as the OSL signal, the stimulation spectrum, the dose dependence, multireadability and short-term fading. Upon optical stimulation in a broad band region from 420 nm to 550 nm with maximum at 435 nm (Bulur & Göksu, 1998), the stimulated luminescence of BeO is generally assumed to be in the same region as that of the thermoluminescence, i.e. UV region with main peak at around 335 nm (McKeever et al., 1995). The exact origin of the optically stimulated luminescence of BeO is not clear yet, although a possible link to the thermoluminescence peaks at 220 °C and 340 °C has been proposed (Bulur & Göksu, 1998). The linear dose response of the optically stimulated luminescence of BeO was reported from 1 μGy up to a few Gy, covering more than six orders of magnitude (Sommer et al., 2008). In practical applications of BeO in radiation dosimetry, the stimulation is usually realized by employing blue light-emitting diodes and the detection of the light can be easily achieved with a photomultiplier. Optical filters are usually used in front of the photomultiplier to discriminate the stimulation light from photostimulated luminescence. The main problem associated with BeO materials is the relatively low reproducibility but in particular the very high toxicity.

2.4 Photoluminescent storage phosphors

Radiophotoluminescent materials and photoluminescent storage phosphors are based on an alteration of the luminescence spectrum of a material upon exposure to ionizing radiation. The phenomenon was reported as early as 1912 by Goldstein (Goldstein, 1912) but it was only in the 1950s that it was realized that the effect could be used for dosimetry (Schulman et al., 1953; Schulman, 1950; Schulman & Etzel, 1953; Schulman et al., 1951). Schulman's system comprised of a silver-activated aluminophosphate glass. Upon exposure to ionizing radiation, electrons are promoted to the conduction band and migrate to the silver activation sites in this system, yielding a reduction of the silver atoms. This reduction results in orange luminescence that can be excited at 365 nm. The main difference to photostimulable materials is the fact that in photoluminescent storage phosphors the radiation-induced change persists upon photoexcitation. For example, if stable colour centres are induced, they can be repetitively read out by photoexcitation whereas in optically stimulable materials *one* radiation induced centre, e.g. electron-hole pair, is annihilated upon the absorption of *one* photon. A study from 1984 suggests the application of rare earth ion co-doped CaSO$_4$ to produce a radiophotoluminescent material at room temperature that also exhibits thermoluminescence i.e. a combined TL/RPL dosimetry system (Calvert & Danby, 1984). In

particular, Eu^{2+} ions if illuminated by ultraviolet radiation display radiophotoluminescence after exposure to ionizing radiation. However, the low sensitivity turned out to be a very limiting factor for this material.

2.4.1 Nanocrystalline BaFCl:Sm^{3+}

Nanocrystalline BaFCl:Sm^{3+}, as prepared by a facile co-precipitation method, is a very efficient photoluminescent storage phosphor for ionizing radiation (Liu et al., 2010; Riesen & Kaczmarek, 2007). The mechanism is based on the reduction of Sm^{3+} to Sm^{2+} by trapping electrons that are created upon exposure to ionizing radiation in the BaFCl host; subsequently, the Sm^{2+} can be efficiently read out by measuring the intraconfigurational *f-f* transitions, such as the $^5D_0$-$^7F_0$ line at around 688 nm, by excitation into the parity allowed $4f^6 \rightarrow 4f^5 5d$ transition at around 415 nm. The latter wavelength is ideal for efficient excitation by blue-violet laser diodes or LEDs as the transition is electric dipole allowed and thus very intense.

The photoluminescence and excitation spectra of nanocrystalline BaFCl:Sm^{3+} after exposure to 50 mGy of 60 kVp X-ray are illustrated in Figure 9. The spectra are dominated by the Sm^{2+} species that is created by the ionizing radiation. The efficiency of this class of storage phosphors can be optimized by the preparation of core-shell nanoparticles comprising of a BaFCl core and a BaFCl:Sm^{3+} shell. The $Sm^{3+} \rightarrow Sm^{2+}$ conversion efficiency of these nanoparticles is drastically higher than that of microcrystals obtained by conventional high temperature (HT) sintering. This is illustrated in Figure 10 where the 415 nm excited luminescence spectra of HT and nanocrystalline BaFCl:Sm^{3+} are compared.
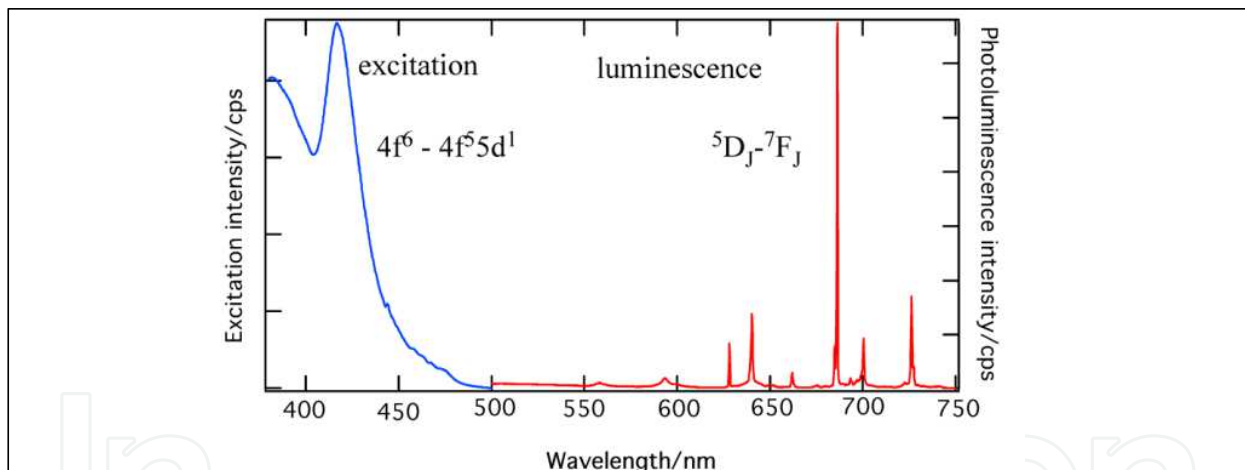

Fig. 9. Photoluminescence and excitation spectra of nanocrystalline BaFCl:Sm^{3+} after exposure to 50 mGy of 60 kVp X-ray radiation. All the pronounced transitions are due to Sm^{2+} which are absent before irradiation. The excitation spectrum is not corrected for the effect of a BG-18 glass filter used for the excitation light.

The HT sample was exposed to a 240,000 times higher radiation dose (12000 Gy) than the nanocrystalline material (50 mGy). It is noted here that there are significant differences in the $^4G_J \rightarrow ^6H_J$ emission lines for the two materials, indicating a significantly different local environment for the Sm^{3+} ions in the nanocrystalline material. It is also clear that both materials provide a range of sites for the Sm^{3+} ions and in the case of the HT material it is straightforward to achieve high site selectivity when changing the excitation wavelength in the vicinity of 400 nm. Nevertheless, after the reduction to Sm^{2+} the resulting $^5D_J \rightarrow ^7F_J$ emission lines perfectly coincide for both materials.
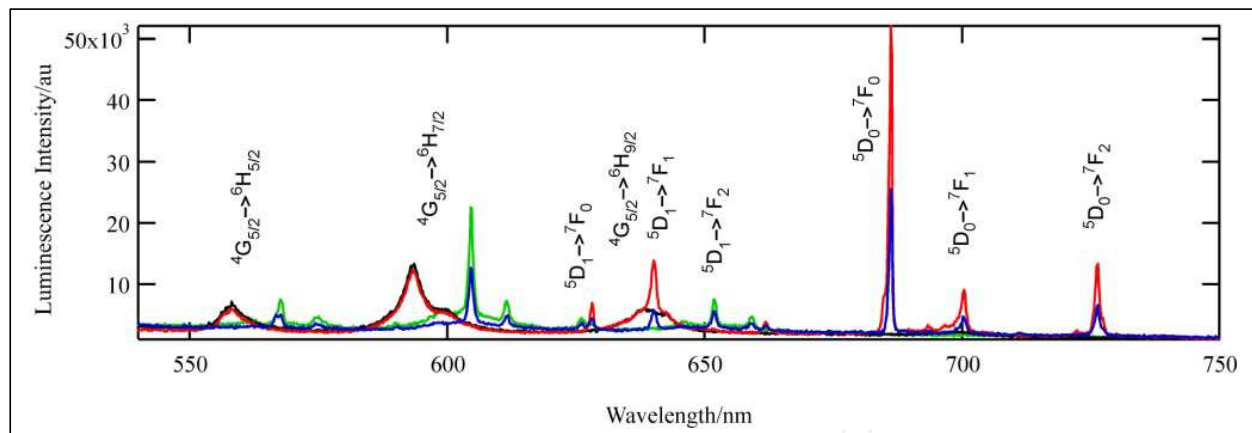
Fig. 10. Photoluminescence of high temperature (green and blue lines) and nanocrystalline (black and red lines) BaFCl:Sm^{3+} before and after exposure to 12000 Gy and 50 mGy, respectively. Prominent $^4G_J \rightarrow ^6H_J$ (Sm^{3+}) and $^5D_J \rightarrow ^7F_J$ (Sm^{2+}) transitions are denoted. Note that the unexposed samples (green and black lines for HT and nano sample, respectively) do not exhibit any emission lines due to Sm^{2+}.

The much higher conversion efficiency (~500,000 times) of the nanocrystalline material manifests itself also in cathodoluminescence where the Sm^{3+} and Sm^{2+} peaks dominate in the spectra of the HT sintered and nanocrystalline samples, respectively (Stevens-Kalceff et al., 2010). The nanocrystalline material has been characterized with a range of techniques such as electron microscopy and high resolution synchrotron powder X-ray diffraction. The diffraction lines in the powder X-ray diffraction pattern can be indexed to the tetragonal matlockite-type structure with space group P4/nmm. The resulting lattice parameters ($a = b$ = 4.395(1) Å, and c = 7.227(8) Å) indicate a small expansion of the crystal lattice in comparison with the literature values (Beck, 1976). The average volume-weighted column length of the crystallites is estimated to be 160 nm by applying the Williamson-Hall procedure (Williamson & Hall, 1953). This average size is consistent with electron microscopy micrographs and renders the nanocrystals for applications where extremely small probes for ionizing radiation are required. For example, if bonded or embedded to/in the end of an optical fibre the material can be used for remote sensing of CW or pulsed ionizing radiation; examples of such applications include real time in vivo monitoring of dose in radiotherapy and in food irradiation and the monitoring of hot labs and/or nuclear reactor environments. In such applications a selected Sm^{2+} emission line, e.g. $^5D_0 \rightarrow ^7F_0$, is monitored with a narrow bandpass filter (e.g. 1 nm FWHM) with gated detection 180^0 out of phase from the excitation light pulse. The latter is facilitated by the relatively long lifetime of 2 ms of the $^5D_0$ excited state and dramatically reduces the lower detection limit by elimination of excitation light, fluorescence due to other impurities and surface defects, and Raman scattered light.

The core-shell nanocrystalline storage phosphor displays a relatively linear response to ionizing radiation up to a surface dose of ca. 10 Gy in the 50 keV X-ray region as is illustrated in Figure 11. Moreover, the lower detection limits for 50 keV and 1 MeV radiation are about 100 nGy and 10 μGy, respectively. This results in an impressive dynamic range of about seven orders of magnitude for radiation detection. A range of photon-gated spectral hole-burning experiments at low temperatures has also been conducted (Liu et al., 2010). The stored energy in the phosphor material can be released by a two-step photoionization process when higher light powers are used. However, the storage phosphor can only be

fully restored after exposures of up to 10-20 mGy. An example of the reproducibility of the nanocrystalline BaFCl:Sm^{3+} for dosimetry applications is illustrated in Figure 12. In this example the Sm^{2+} photoluminescence signal was measured as a function of accumulated dose (60 kVp X-ray irradiation) up to 1 mGy. The dosimeter material was then bleached by a two-step photoionization and the experiment was repeated. As follows from this figure, the phosphor can be fully restored in this range of absorbed doses.
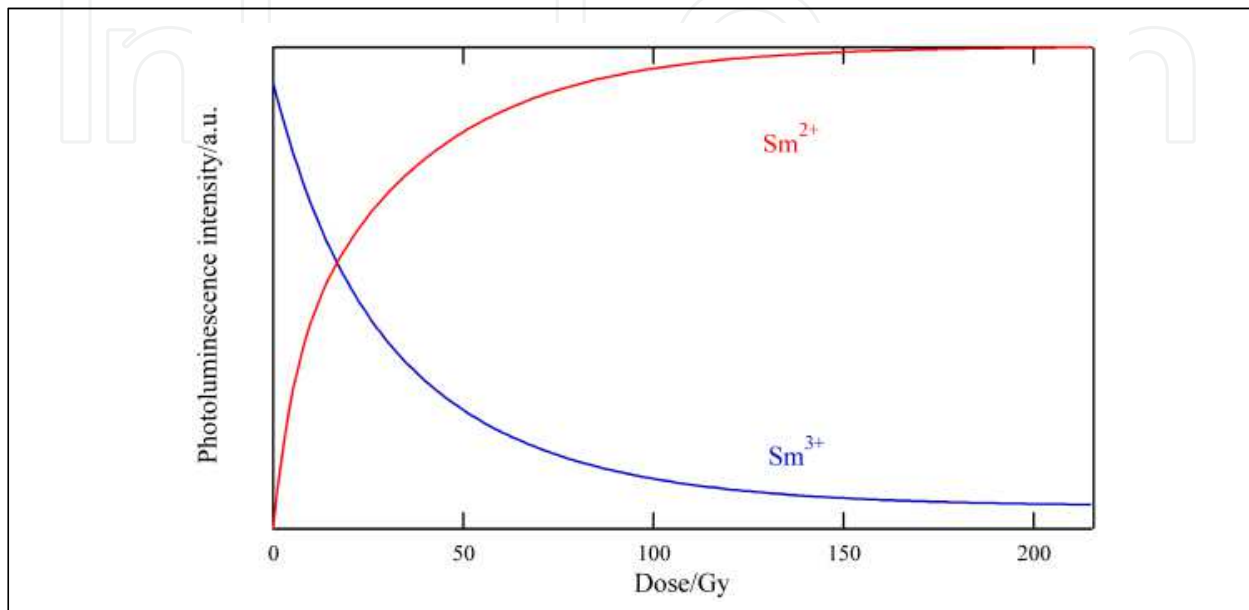
Fig. 11. Dependence of the Sm^{2+} and Sm^{3+} photoluminescence signals of nanocrystalline BaFCl:Sm^{3+} on absorbed 60 kVp X-ray dose.
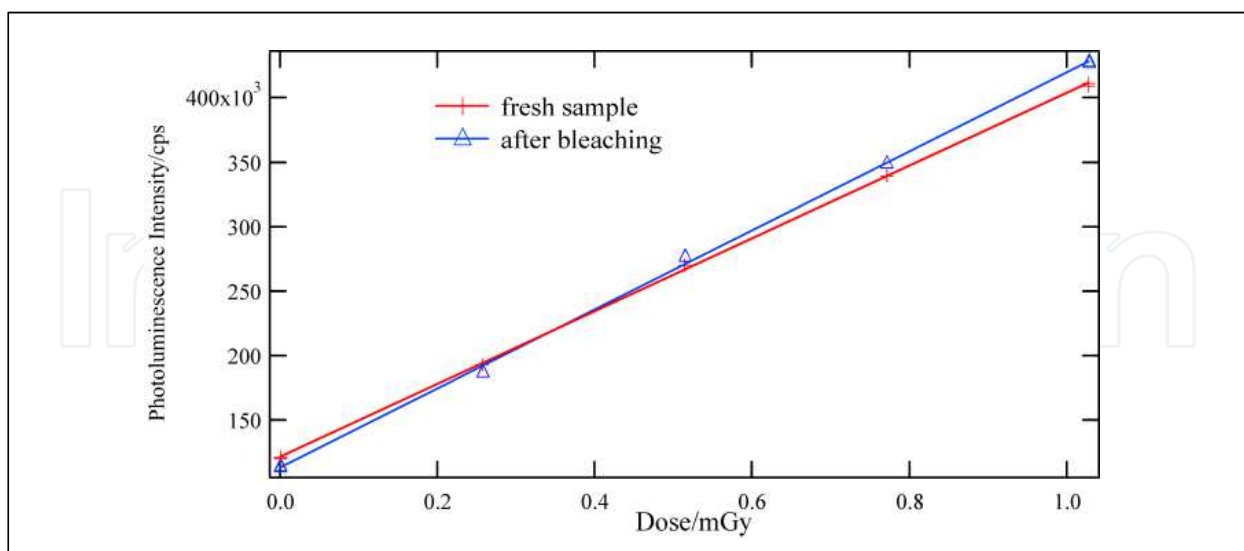
Fig. 12. Reproducibility of nanocrystalline BaFCl:Sm^{3+} in dosimetry.

Figure 13 illustrates the dose dependence of the Sm^{2+} photoluminescence signal upon exposure to Cs-137 γ-rays (662 keV). The phosphor's response is independent on the dose rate and fairly linear up to the maximum exposure of ca ~10 mGy.
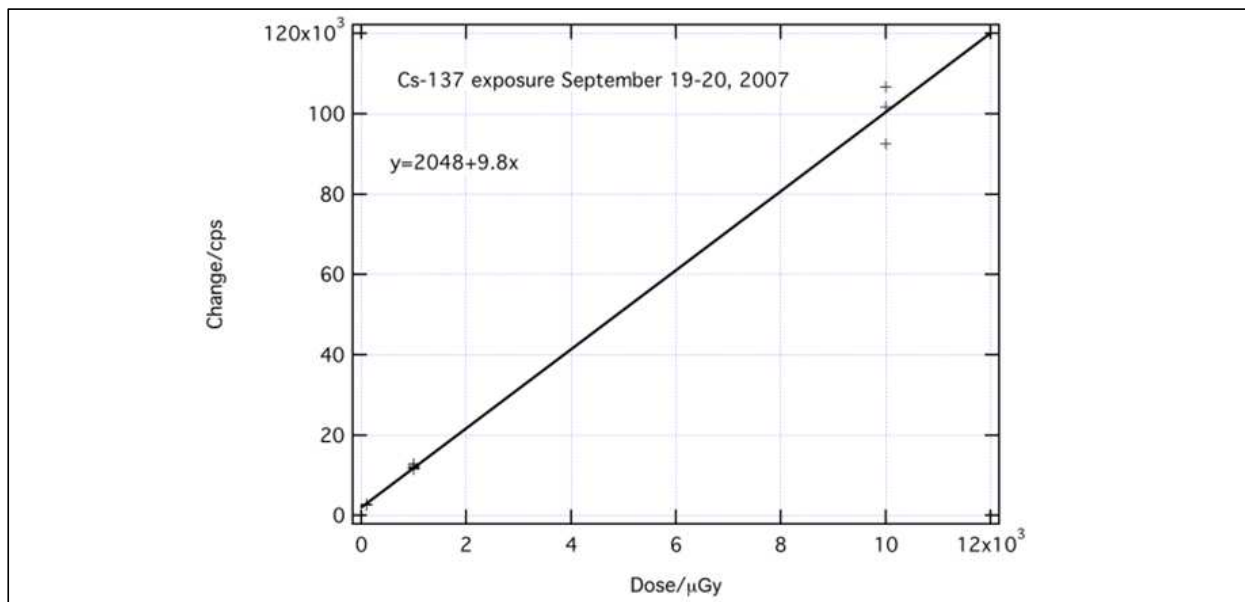
Fig. 13. Dependence of the Sm^{2+} photoluminescence intensity on absorbed dose of Cs-137 γ-rays (662 keV)

As can be expected, due to the presence of heavy atoms in the $BaFCl:Sm^{3+}$ material, the phosphor's quantum efficiency is subject to a relatively strong energy dependence. This is illustrated in Figure 14. As a consequence, if used in dosimetry, filters need to be applied. However, the strong energy dependence together with a filter arrangement allows the determination of the energy of the ionizing radiation, a desirable feature.
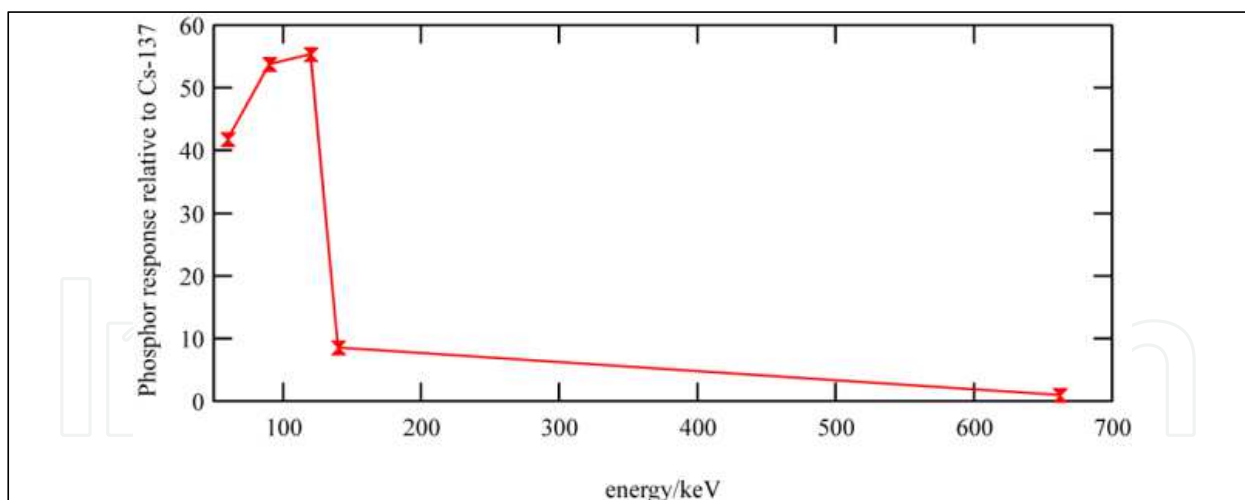
Fig. 14. Energy dependence of the conversion efficiency of nanocrystalline $BaFCl:Sm^{3+}$ relative to Cs-137 γ-rays (662 keV).

The lifetime of the excited ^5D_J multiplet is about 2 ms which is a severe limitation in computed radiography when the conventional "flying-spot" readout scheme is applied. However, the long lifetime allows for gated excitation and luminescence light with a phase shift of 180°. The gated readout facilitates a very sensitive detection scheme since fluorescence of impurities is blocked from reaching the light detector. A big advantage of the nanocrystalline $BaFCl:Sm^{3+}$ phosphor is the submicron particle size that increases the

spatial resolution which, in the commercial BaFBr(I):Eu^{2+} is limited by the large grain size that induces significant light scattering in the readout process. The nanocrystalline BaFCl:Sm^{3+} also allows a higher packing density and the light scattering in the readout process can be expected to be a lesser problem. This can be tested by determining the modulation transfer function (MTF). The MTF can be determined following the procedure outlined in Figure 15 (Boone, 2001; Cunningham & Fenster, 1987; Cunningham & Reid, 1992; Samei et al., 1998; Samei et al., 2001). In particular, in the first step the edge spread function (ESF) is measured, by imaging a lead edge. The line spread function (LSF) is then calculated by differentiating the ESF and subsequently the MTF is obtained by Fast Fourier Transformation of the LSF. Thin films of nanocrystalline BaFCl:Sm^{3+} were applied to a plastic substrate by mixing the phosphor with a small amount of polyvinyl acetate. A 2D reader unit that images the excited photoluminescence of the BaFCl:Sm^{3+} storage plate by an electron-multiplying CCD (EMCCD) camera was employed to image the plate in parallel mode. The system relies on gated excitation-detection by pulsing the LEDs and mechanically gating the collimated luminescence light by a mechanical chopper wheel. This prevents fluorescence of impurities from reaching the detector. The 2D reader unit is illustrated in Figure 15 where the LED light sources, the film platform, the lens system, the chopper wheel and the EMCCD camera can be recognized.
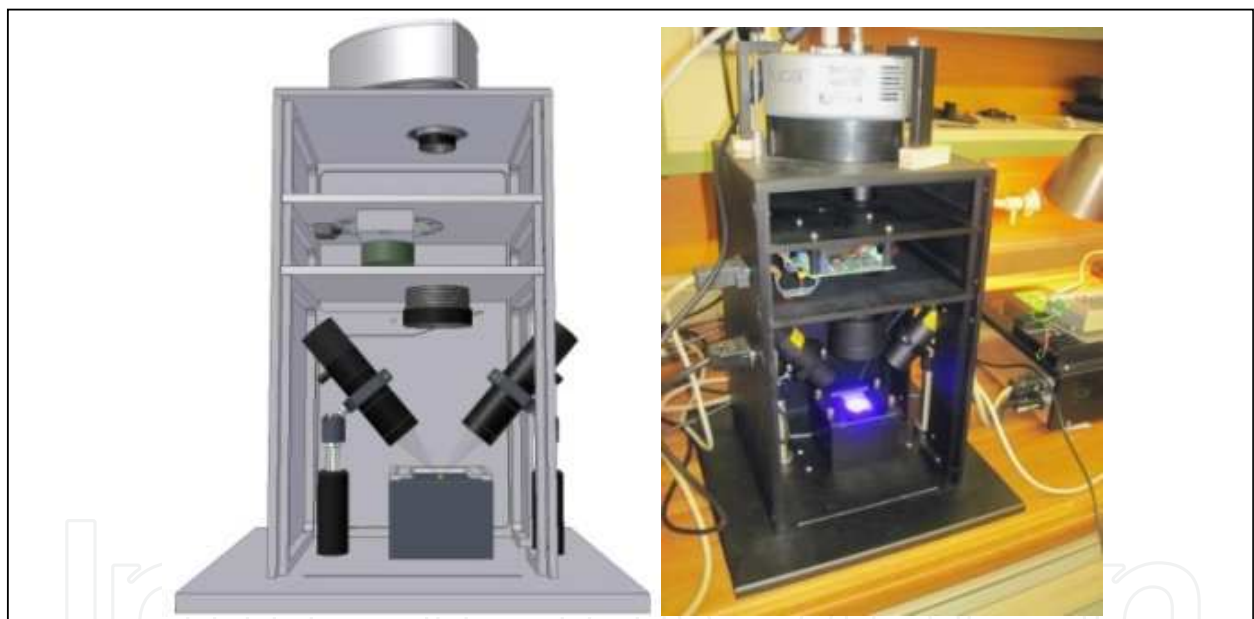

Fig. 15. 2D reader for imaging plates based on nanocrystalline BaFCl:Sm^{3+}. The image plate is illuminated by two collimated and pulsed 405 nm mounted blue LEDs. The emitted light is collimated then passed through an aperture, that is opened with a 180° phase shift with respect to the blue LED pulses, by a mechanical light chopper wheel. The light is then refocused, filtered and detected by an EMCCD camera.

Radiographs were analyzed according to the mathematical steps shown in Figure 16. In particular, the line spread function (LSF) is obtained from the edge spread function (ESF) by differentiation and the MTF by Fast Fourier Transformation (FFT) of the LSF.

$$LSF(x) = \frac{d}{dx} ESF(x) \qquad (1)$$

$$MTF(k) = \int_{-\infty}^{\infty} LSF(x)\exp(-i2\pi kx)dx \qquad (2)$$
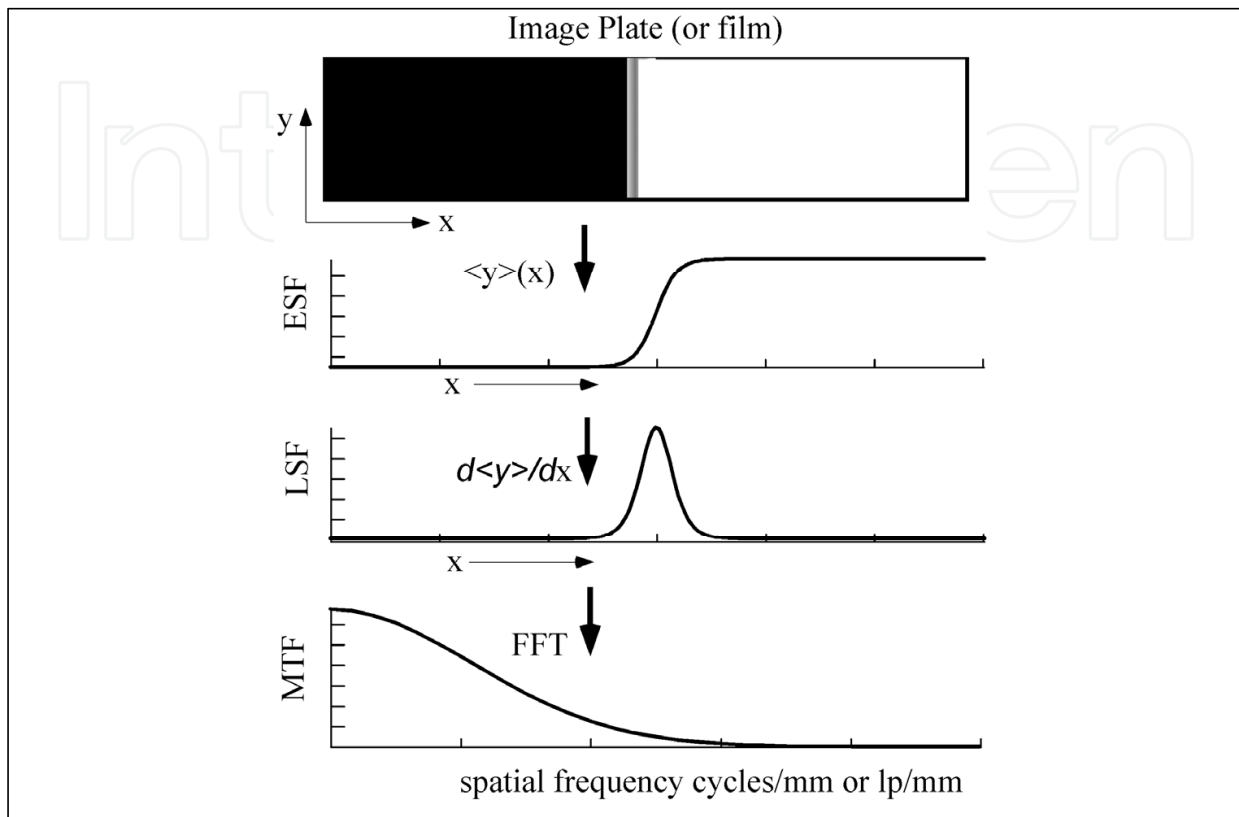
Fig. 16. Procedure to determine the MTF of an optical storage phosphor.

The resulting MTF is illustrated in Figure 17 and, for the purpose of comparison, the MTFs of the Kodak Insight dental film and Kodak GP and HR imaging plates in conjunction with Kodak Ektascan Model-400 and CR9000 computed radiography reader units are shown. The MTF points for the BaFCl:Sm³⁺ imaging plates are calculated from raw data whereas for the smooth green line the ESF is based on a fit of a sigmoid to the ESF and the solid blue line is based on smoothing the ESF with the Savitzky-Golay procedure in 4th order using 37 points.

	BaFCl:Sm^{3+} imaging plate	Kodak CR9000 reader with CR-GP plate	Kodak Ektascan Model-400 reader with GP plate	Kodak Ektascan Model-400 reader with HR plate	Kodak Insight With 2D reader	Kodak Insight with plustek OpticFilm 7400
MTF=0.5	2.4	1.3	1.22	1.92	2.8	4.7
MTF=0.1	5.4	3.1	3.27	4.35	18	18

Table 3. Comparison of MTF values of BaFCl:Sm³⁺ imaging plates with Kodak Computed radiography systems and conventional Kodak Insight dental film.

In Table 3 a comparison of MTF data is compiled, in particular the spatial frequency is summarized at MTF values of 0.5 and 0.1. It is obvious that conventional dental film exhibits by far the best values. However, the BaFCl:Sm^{3+} based imaging plates are significantly better than all the commercial computed radiography systems shown in Table 3. It follows that the nanocrystalline BaFCl:Sm^{3+} storage phosphor yields imaging plates with a better MTF in comparison with commercially available computed radiography systems. It is noted here that a better MTF is highly desirable as it is the main drawback of computed radiography based on currently used storage phosphors. In particular in medical imaging a good MTF is required in order to detect, for example, micro-calcifications in soft tissue. High resolution imaging is also important for a range of scientific and technical imaging applications.
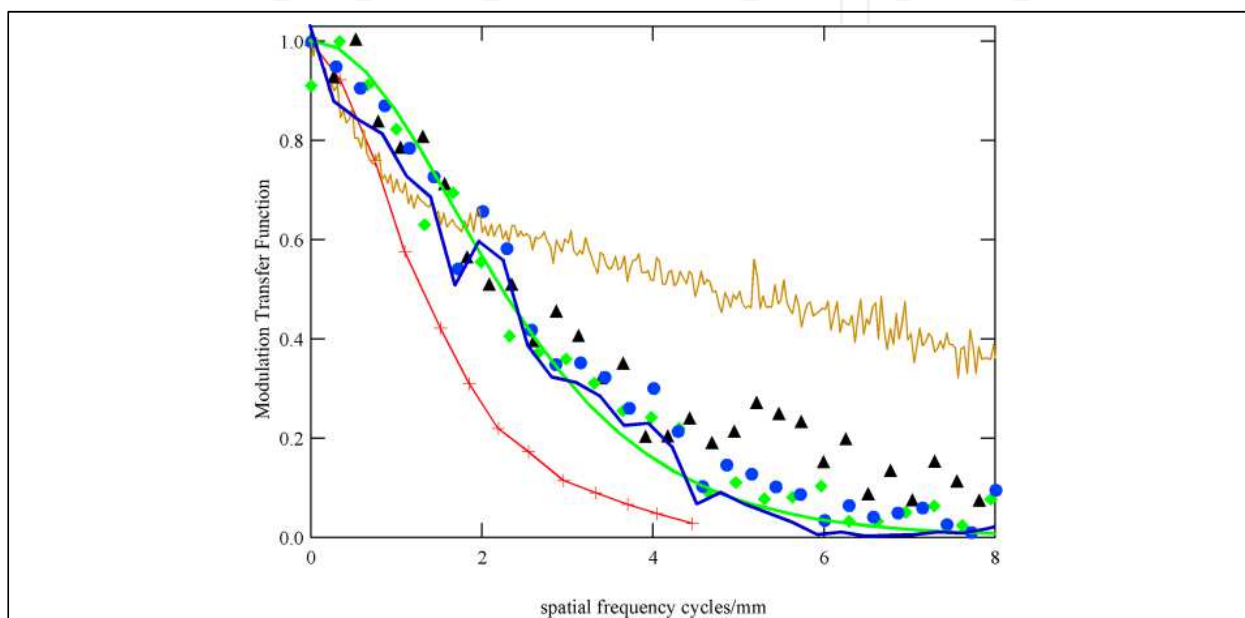

Fig. 17. MTF data for BaFCl:Sm^{3+} based imaging plate (blue solid circles, black solid triangles, green diamonds and green trace). The smooth green line is based on a fit of the ESF to a sigmoid. The blue line is the result of a Savitzky-Golay smoothing procedure applied to the ESF. The red trace with markers is the MTF of the Kodak CR9000 computed radiography system. The beige trace is the MTF of Kodak Insight dental film as read out by the 2D reader unit illustrated in Figure 15.

3. Conclusion

Over the last 60 years an impressive range of optical storage phosphors and materials has been developed and investigated for a plethora of applications, including personal radiation monitoring, quality control in radiation therapy and food irradiation, and for applications in computed radiography both for medical and technical applications. Although full electronic devices, both for point and 2D detection, are becoming increasingly more sensitive and inexpensive, many applications for optical storage phosphors prevail, possible for many years to come, as electronic solid state devices are not flexible and hence for many applications not practical. Importantly, storage phosphor based dosimeters are always accumulating and independent of any power supply. Optical storage phosphors have a significant potential to facilitate much lower radiation doses in medical imaging, a highly desirable outcome.

4. Acknowledgment

5. References

AbdelFattah, A.A. & Miller, A. (1996). Temperature, Humidity and Time. Combined Effects on Radiochromic Film Dosimeters. *Radiation Physics and Chemistry,* Vol. 47, No. 4, 611-621.

Akselrod, M.S., Kortov, V.S., Kravetsky, D.J. & Gotlib, V.I. (1990). Highly Sensitive Thermoluminescent Anion-Defective α-Al$_2$O$_3$:C Single Crystal Detectors. *Radiation Protection Dosimetry,* Vol. 32, No. 1, 15-20.

Akselrod, M.S., Lucas, A.C., Polf, J.C. & McKeever, S.W.S. (1998). Optically Stimulated Luminescence of Al$_2$O$_3$. *Radiation Measurements,* Vol. 29, No. 3-4, 391-399, 1350- 4487.

Akselrod, M.S. (2011). Fundamentals of Materials, Techniques, and Instrumentation for OSL and FNTD Dosimetry, *AIP Conference Proceedings*, Sydney, Australia, September 2010.

Albrecht, H. & Mandeville, C. (1956). Storage of Energy in Beryllium Oxide. *Physical Review,* Vol. 101, No. 4, 1250-1252.

Andersen, C.E., Nielsen, S.K., Greilich, S., Helt-Hansen, J., Lindegaard, J.C. & Tanderup, K. (2009). Characterization of a Fiber-Coupled Al$_2$O$_3$:C Luminescence Dosimetry System for Online in Vivo Dose Verification During [192]Ir Brachytherapy. *Medical Physics,* Vol. 36, No. 3, 708-718, 0094-2405.

Appleby, G., Zimmermann, J., Hesse, S., Karg, O. & von Seggern, H. (2009). Sensitization of the Photostimulable X-ray Storage Phosphor CsBr: Eu^{2+} Following Room-Temperature Hydration. *Journal of Applied Physics,* Vol. 105, No. 7, 0735111-0735115, 0021-8979.

Arjomandy, B., Tailor, R., Anand, A., Sahoo, N., Gillin, M., Prado, K. & Vicic, M. (2010). Energy Dependence and Dose Response of Gafchromic EBT2 Film Over a Wide Range of Photon, Electron, and Proton Beam Energies. *Medical Physics,* Vol. 37, No. 1942-1947.

Azorin, J., Furetta, C. & Scacco, A. (1993). Preparation and Properties of Thermoluminescent Materials. *physica status solidi (a),* Vol. 138, No. 1, 9-46, 1521-396X.

Beck, H. (1976). A Study on Mixed Halide Compounds MFX (M= Ca, Sr, Eu, Ba; X= Cl, Br, I). *Journal of Solid State Chemistry,* Vol. 17, No. 3, 275-282, 0022-4596.

Boone, J.M. (2001). Determination of the Presampled MTF in Computed Tomography. *Medical Physics,* Vol. 28, No. 356-360.

Borgman, I.L. (1897). Thermoluminescence Provoquee par les Rayons de M. Roentgen et les Rayons de M. Becquerel. *Comptes Rendus,* Vol. 124, No. 895-896,

Bos, A. (2001). High Sensitivity Thermoluminescence Dosimetry. *Nuclear Instruments and Methods in Physics Research Section B: Beam Interactions with Materials and Atoms,* Vol. 184, No. 1-2, 3-28, 0168-583X.

Bøtter-Jensen, L., McKeever, S.W.S. & Wintle, A.G. (2003). *Optically Stimulated Luminescence Dosimetry, Elsevier Science, Amsterdam; Boston; London.*

Bulur, E. & Göksu, H. (1998). OSL From BeO Ceramics: New Observations from an Old Material. *Radiation Measurements,* Vol. 29, No. 6, 639-650, 1350-4487.

Butson, M.J., Yu, P.K.N., Cheung, T. & Alnawaf, H. (2010). Energy Response of the New EBT2 Radiochromic Film to X-ray Radiation. *Radiation Measurements,* Vol. 45, No. 7, 836-839, 1350-4487.

Calvert, R. & Danby, R. (1984). Thermoluminescence and Radiophotoluminescence From Eu- and Sm-Doped CaSO₄. *physica status solidi (a),* Vol. 83, No. 2, 597-604, 1521- 396X.

Crase, K. & Gammage, R. (1975). Improvements in the Use of Ceramic BeO for TLD. *Health Physics,* Vol. 29, No. 5, 739-746, 0017-9078.

Cunningham, I. & Fenster, A. (1987). A Method for Modulation Transfer Function Determination from Edge Profiles with Correction for Finite-Element Differentiation. *Medical Physics,* Vol. 14, No. 4, 533–537.

Cunningham, I. & Reid, B. (1992). Signal and Noise in Modulation Transfer Function Determinations Using the Slit, Wire, and Edge Techniques. *Medical Physics,* Vol. 19, No. 1037-1044.

Daniels, F., Boyd, C.A. & Saunders, D.F. (1953). Thermoluminescence as a Research Tool. *Science,* Vol. 117, No. 3040, 343-349, 0036-8075.

Dyk, J.V. (1999). *The Modern Technology of Radiation Oncology: A Compendium for Medical Physicists and Radiation Oncologists,* Medical Physics Publishing, 9780944838389, Madison, Wisconsin.

Eichholz, G.G. (2003). Dosimetry for Food Irradiation. *Health Physics,* Vol. 84, No. 5, 665, 0017-9078.

Goldstein, E. (1912). Concerning the Emission Spectra of Aromatic Bonds in Ultra Violet Light, in Cathode Rays, Radium Radiation and Positive Rays. *Pysikalische Zeitschrift,* Vol. 13, No. 188-193.

Hackenschmied, P., Zeitler, G., Batentschuk, M., Winnacker, A., Schmitt, B., Fuchs, M., Hell, E. & Knüpfer, W. (2002). Storage Performance of X-ray Irradiated Doped CsBr. *Nuclear Instruments and Methods in Physics Research Section B: Beam Interactions with Materials and Atoms,* Vol. 191, No. 1-4, 163-167, 0168-583X.

Hackenschmied, P., Schierning, G., Batentschuk, M. & Winnacker, A. (2003). Precipitation-induced Photostimulated Luminescence in CsBr: Eu^{2+}. *Journal of Applied Physics,* Vol. 93, No. 9, 5109-5112, 0021-8979.

Hangleiter, T., Koschnick, F. & Spaeth, J. (1990). Temperature Dependence of the Photostimulated Luminescence of X-irradiated BaFBr: Eu^{2+}. *Journal of Physics: Condensed Matter,* Vol. 2, No. 32, 6837-6846.

Horowitz, Y.S. (1984). *Thermoluminescence and Thermoluminescent Dosimetry,* CRC Press, 9780849356650 Boca Raton, FL.

Kortov, V. (2007). Materials for Thermoluminescent Dosimetry: Current Status and Future Trends. *Radiation Measurements,* Vol. 42, No. 4-5, 576-581, 1350-4487.

Koschnick, F.K., Spaeth, J.M., Eachus, R.S., McDugle, W.G. & Nuttall, R.H.D. (1991). Experimental Evidence for the Aggregation of Photostimulable Centers in BaFBr:Eu^{2+} Single Crystals by Cross Relaxation Spectroscopy. *Physical Review Letters,* Vol. 67, No. 25, 3571-3574, 0031-9007.

Leblans, P.J.R., Struye, L. & Willems, P. (2001). New Needle-Crystalline CR Detector, *Procccedings of SPIE* San Diego, CA, USA, February 2001.

Lewis, D.F. (1986). A Processless Electron Recording Medium, *Proceedings of SPSE'86 Symposium*, Arlington, VA.

Liu, Z., Massil, T. & Riesen, H. (2010). Spectral Hole-Burning Properties of Sm^{2+} ions. Generated by X-rays in BaFCl: Sm^{3+} Nanocrystals. *Physics Procedia,* Vol. 3, No. 4, 1539-1545, 1875-3892.

McKeever, J., Walker, F. & McKeever, S. (1993). Properties of the Thermoluminescence Emission from LiF (Mg, Cu, P). *Nuclear Tracks and Radiation Measurements,* Vol. 21, No. 1, 179-183, 0969-8078.

McKeever, S.W.S. (1988). *Thermoluminescence of Solids,* Cambridge University Press, 0521368111, Cambridge, New York.

McKeever, S.W.S., Moscovitch, M. & Townsend, P.D. (1995). *Thermoluminescence Dosimetry Materials: Properties and Uses,* Nuclear Technology Publishing, 1870965191, England.

Mclaughlin, W.L., Yundong, C., Soares, C.G., Miller, A., Vandyk, G. & Lewis, D.F. (1991). Sensitometry of the Response of a New Radiochromic Film Dosimeter to Gamma-Radiation and Electron-Beams. *Nuclear Instruments & Methods in Physics Research Section a-Accelerators Spectrometers Detectors and Associated Equipment,* Vol. 302, No. 1, 165-176, 0168-9002.

Mijnheer, B. (2008). State of the Art of in vivo Dosimetry. *Radiation Protection Dosimetry,* Vol. 131, No. 1, 117-122, 0144-8420.

Milman, I., Sjurdo, A., Kortov, V. & Lesz, J. (1996). TSEE and TL of Non-Stoichiometric BeO-TiO$_2$ Ceramics. *Radiation Protection Dosimetry,* Vol. 65, No. 1-4, 401, 0144-8420.

Nakajima, T., Murayama, Y., Matsuzawa, T. & Koyano, A. (1978). Development of a New Highly Sensitive LiF Thermoluminescence Dosimeter and its Applications. *Nuclear Instruments and Methods,* Vol. 157, No. 1, 155-162, 0029-554X.

Nakano, Y., Gido, T., Honda, S., Maezawa, A., Wakamatsu, H. & Yanagita, T. (2002). Improved Computed Radiography Image Quality from a BaFI: Eu Photostimulable Phosphor Plate. *Medical Physics,* Vol. 29, No. 592-597.

Paul, J.R.L., Willems, P. & Alaerts, L.B. (2002). New Needle-Crystalline Detector For X-Ray Computer Radiography (CR). *The e-Journal of Nondestructive Testing,* Vol. 7, No. 12, 1435-4934.

Podgorsak, E. (2005). *Radiation Oncology Physics: A Handbook for Teachers and Students,* International Atomic Energy Agency, 9201073046, Vienna.

Riesen, H. & Kaczmarek, W.A. (2005). *Radiation Storage Phosphor & Applications,* International PCT Application PCT/AU2005/001905, International Publication Number WO 2006/063409.

Riesen, H. & Kaczmarek, W.A. (2007). Efficient X-ray Generation of Sm^{2+} in Nanocrystalline BaFCl/Sm^{3+}: A Photoluminescent X-ray Storage Phosphor. *Inorganic Chemistry,* Vol. 46, No. 18, 7235-7237, 0020-1669.

Riesen, H. & Piper, K. (2008). *Apparatus and Method for Detecting and Monitoring Radiation,* International PCT application.

Rink, A., Lewis, D.F., Varma, S., Vitkin, I.A. & Jaffray, D.A. (2008). Temperature and Hydration Effects on Absorbance Spectra and Radiation Sensitivity of a Radiochromic Medium. *Medical Physics,* Vol. 35, No. 4545-4555.

Samei, E., Flynn, M.J. & Reimann, D.A. (1998). A Method for Measuring the Presampled MTF of Digital Radiographic Systems Using an Edge Test Device. *Medical Physics,* Vol. 25, No. 102-113.

Samei, E., Seibert, J.A., Willis, C.E., Flynn, M.J., Mah, E. & Junck, K.L. (2001). Performance Evaluation of Computed Radiography Systems. *Medical Physics,* Vol. 28, No. 361- 371.

Satinger, D., Horowitz, Y.S. & Oster, L. (1999). Isothermal Decay of Isolated Peak 5 in 165degC/15 Minute Post-Irradiation Annealed LiF:Mg,Ti (TLD-100) Following Alpha Particle and Beta Ray Irradiation. *Radiation Protection Dosimetry,* Vol. 84, No. 1-4, 67-72.

Schulman, J., Shurcliff, W., Ginther, R. & Attix, F. (1953). Radiophotoluminescence Dosimetry System of the US Navy. *Nucleonics (U.S.) Ceased publication,* Vol. 11, No. 10, 52-56.

Schulman, J.H. (1950). *Dosimetry of X-rays and Gamma Rays.*, Naval Research Laboratory. Report No. 3736, Washington, DC.

Schulman, J.H., Ginther, R.J., Klick, C.C., Alger, R.S. & Levy, R.A. (1951). Dosimetry of X-Rays and Gamma-Rays by Radiophotoluminescence. *Journal of Applied Physics,* Vol. 22, No. 12, 1479-1487, 0021-8979.

Schulman, J.H. & Etzel, H.W. (1953). Small-Volume Dosimeter for X-Rays and Gamma-Rays. *Science,* Vol. 118, No. 3059, 184-186, 0036-8075.

Schweizer, S., Rogulis, U., Assmann, S. & Spaeth, J.M. RbBr and CsBr Doped with Eu²⁺ As New Competitive X-ray Storage Phosphors, *Proceedings of the Fifth International Conference on Inorganic Scintillators and their Applications*, 1350-4487, Riga-Jurmala, Latvia, August 2000.

Schweizer, S. (2001). Physics and Current Understanding of X-Ray Storage Phosphors. *physica status solidi (a),* Vol. 187, No. 2, 335-393, 1521-396X.

Schweizer, S., Secu, M., Spaeth, J.M., Hobbs, L., Edgar, A. & Williams, G. (2004). New Developments in X-ray Storage Phosphors. *Radiation Measurements,* Vol. 38, No. 4-6, 633-638, 1350-4487.

Secerov, B., Dakovic, M., Borojevic, N. & Bacic, G. (2011). Dosimetry Using HS GafChromic Films the Influence of Readout Light on Sensitivity of Dosimetry. *Nuclear Instruments & Methods in Physics Research Section a-Accelerators Spectrometers Detectors and Associated Equipment,* Vol. 633, No. 1, 66-71, 0168-9002.

Soares, C.G. (2006). New Developments in Radiochromic Film Dosimetry. *Radiation Protection Dosimetry,* Vol. 120, No. 1-4, 100-106, 0144-8420.

Soares, C.G. (2007). Radiochromic Film Dosimetry. *Radiation Measurements,* Vol. 41, No. Supplement 1, S100-S116, 1350-4487.

Sommer, M., Jahn, A. & Henniger, J. (2008). Beryllium Oxide as Optically Stimulated Luminescence Dosimeter. *Radiation Measurements,* Vol. 43, No. 2-6, 353-356, 1350-4487.

Stevens-Kalceff, M.A., Riesen, H., Liu, Z., Badek, K. & Massil, T. (2010). Microcharacterization of Core Shell Nanocrystallites. *Microscopy and Microanalysis,* Vol. 16, No. S2, 1818-1819, 1435-8115.

Takahashi, K., Kohda, K., Miyahara, J., Kanemitsu, Y., Amitani, K. & Shionoya, S. (1984). Mechanism of Photostimulated Luminescence in BaFX:Eu²⁺ (X=Cl,Br) Phosphors. *Journal of Luminescence,* Vol. 31-32, No. PART 1, 266-268.

Vij, D.R. & Singh, N. (1997). Thermoluminescence Dosimetric Properties of Beryllium Oxide. *Journal of Materials Science,* Vol. 32, No. 11, 2791-2796, 0022-2461.

von Seggern, H. (1999). Photostimulable X-ray Storage Phosphors: A Review of Present Understanding. *Brazilian journal of physics,* Vol. 29, No. 2, 254-268, 0103-9733.

Weidner, M., Batentschuk, M., Meister, F., Osvet, A., Winnacker, A., Tahon, J.P. & Leblans, P. (2007). Luminescence Spectroscopy of Eu²⁺ in CsBr: Eu Needle Image Plates (NIPs). *Radiation Measurements,* Vol. 42, No. 4-5, 661-664, 1350-4487.

Williamson, G. & Hall, W. (1953). X-Ray Line Broadening From Filed Aluminium and Wolfram. *Acta Metallurgica,* Vol. 1, No. 1, 22-31, 0001-6160.

Yamashit, T. Yasuno, Y. & Ikedo, M. (1974). Beryllium-Oxide Doped with Lithium or Sodium for Thermoluminescence Dosimetry. *Health Physics,* Vol. 27, No. 2, 201-206, 0017-9078.

Yen, W.M., Shionoya, S. & Yamamoto, H. (2007). *Phosphor Handbook, (second edition)*, CRC, 0849335647, Boca Raton, FL.

Zimmermann, J., Hesse, S., von Seggern, H., Fuchs, M. & Knüpfer, W. (2005). Radiation Hardness of CsBr: Eu²⁺. *Journal of Luminescence,* Vol. 114, No. 1, 24-30, 0022-2313.
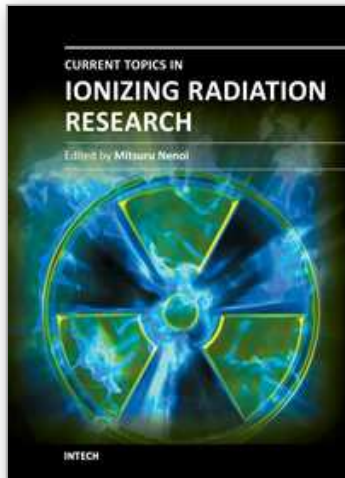
Current Topics in Ionizing Radiation Research

Edited by Dr. Mitsuru Nenoi

Since the discovery of X rays by Roentgen in 1895, the ionizing radiation has been extensively utilized in a variety of medical and industrial applications. However people have shortly recognized its harmful aspects through inadvertent uses. Subsequently people experienced nuclear power plant accidents in Chernobyl and Fukushima, which taught us that the risk of ionizing radiation is closely and seriously involved in the modern society. In this circumstance, it becomes increasingly important that more scientists, engineers and students get familiar with ionizing radiation research regardless of the research field they are working. Based on this idea, the book "Current Topics in Ionizing Radiation Research" was designed to overview the recent achievements in ionizing radiation research including biological effects, medical uses and principles of radiation measurement.

How to reference

In order to correctly reference this scholarly work, feel free to copy and paste the following:

Hans Riesen and Zhiqiang Liu (2012). Optical Storage Phosphors and Materials for Ionizing Radiation, Current Topics in Ionizing Radiation Research, Dr. Mitsuru Nenoi (Ed.), ISBN: 978-953-51-0196-3, InTech, Available from: http://www.intechopen.com/books/current-topics-in-ionizing-radiation-research/optical-storage-phosphors-and-materials-for-ionizing-radiation

INTECH

open science | open minds